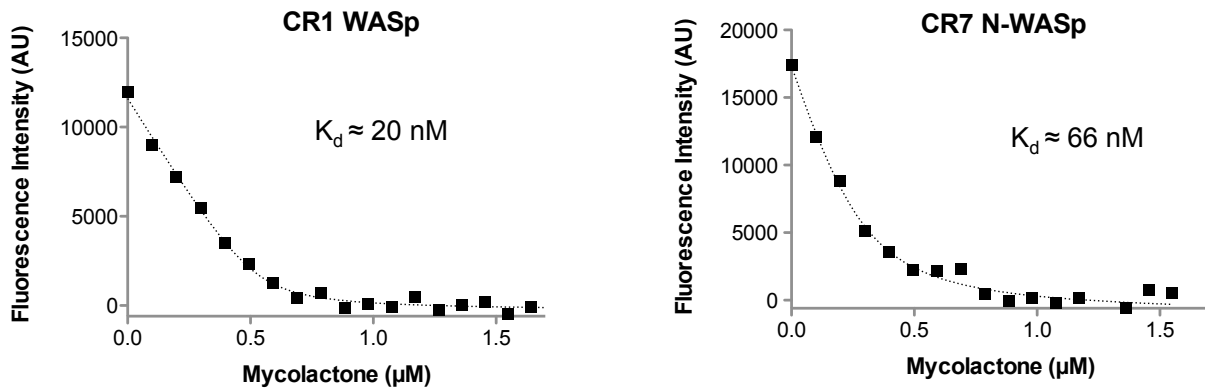


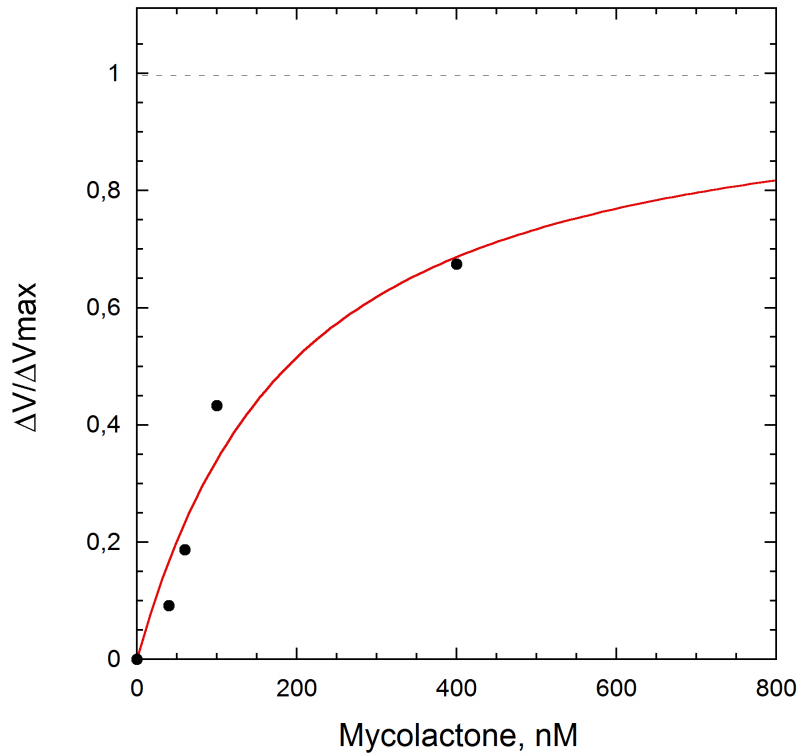
Supplemental Figure 1

Structure and biological activity of biotinylated mycolactone. **(A)** Mycolactone (1 mg) was oxidized by 1 ml NaIO_4 10 mM in $\text{H}_2\text{O}:\text{C}_4\text{H}_8\text{O}$ (tetrahydrofuran) (50:50) for 1 h at RT in the dark, under nitrogen gas flow. The resulting product was extracted by anhydrous ethyl acetate, incubated with anhydrous sodium sulphate for 30 min, then dried under nitrogen gas flow and resuspended in 1 ml $\text{CHCl}_3:\text{MeOH}$ 2:1. Biotin-LC-hydrazide (Pierce, ref 21340) was then added at a molar ratio of 2:1 in DMSO, and the reaction mixture incubated for 2 h at RT in the dark, dried under nitrogen and resuspended in MeOH. The yielded product was purified on BDS Hypersil C8 (250*4.6 mm) (Thermo Electron Corporation) with a $\text{CH}_3\text{CN}/\text{H}_2\text{O}$ gradient of 55% to 95% over 40 min. **(B)** The biological activity of the resulting Myco-biotin molecule, as evaluated by its immunosuppressive activity on activation-induced production of IL-2 by Jurkat T cells and cytotoxic activity on HeLa cells is shown, compared to mycolactone (Myco). The cytopathic activity of mycolactone was determined by MTT [3-(4,5-Dimethylthiazol-2-yl)-2,5-Diphenyltetrazolium Bromide] assay. Briefly, HeLa cells were incubated in 96-well plates (10^4 cells/well) with mycolactone for 48 h, prior to the addition of MTT at 50 $\mu\text{g}/\text{ml}$. After 4 h, culture supernatants were removed and formazan crystals dissolved in DMSO for absorbance measurement. The immunosuppressive activity of mycolactone was measured on Jurkat T cells inoculated in 96-well plates (5×10^5 cells/well) and incubated with mycolactone for 4 h, then stimulated for 20 h with 50 ng/ml PMA and 1 $\mu\text{g}/\text{ml}$ calcium ionophore. Production of IL-2 was assessed in culture supernatants by ELISA (DuoSet, R&D systems).



Supplemental Figure 2

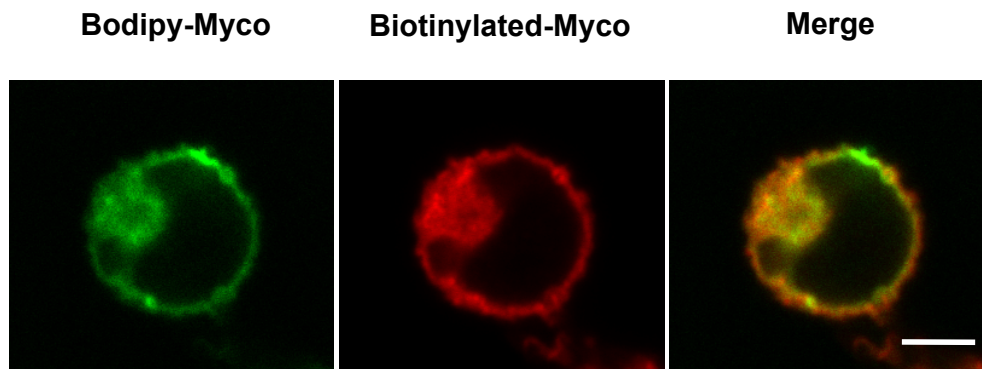
Fluorescence emission of CR1 WASp and CR7 N-WASp in the presence of increasing concentrations of mycolactone. Fluorescence studies were performed on a PTI Quanta-Master QM4CW spectrofluorimeter (PTI, Lawrenceville, NJ) at 25°C using a 10 mm wide quartz cuvette. The excitation wavelength was fixed at 292 nm and intrinsic fluorescence emission of the single tryptophan residues in N-wasp CR7 and Wasp CR1 domain (corresponding to Trp217 and Trp252 in full-length proteins) was recorded at 345 nm. Bandwidths of excitation and emission monochromators were set at 1 and 10 nm, respectively. Cells were charged with 5 μM of either N-WASp CR7 or WASp CR1 in a final volume of 1 ml of purification buffer (20 mM Tris-HCl pH7.5, 100 mM KCl, 1 mM DTT). Purified mycolactone was added step by step to the mixture with a 0.1 μM increment. The fluorescence of mycolactone alone and passive fluorescence of N-WASp CR7 or WASp CR1 were subtracted to each step point. The resultant fluorescence intensity was plotted as a function of mycolactone concentration, and K_d determined by least squares fitting using OriginLab (Northampton, MA). In accordance with previous reports demonstrating that isolated GBDs are largely unstructured in solution, curve-fitting was made under the assumption that 5-10% of the peptides was able to bind mycolactone. AU, arbitrary unit. Comparable results were obtained using two independent protein preparations.



Supplemental Figure 3

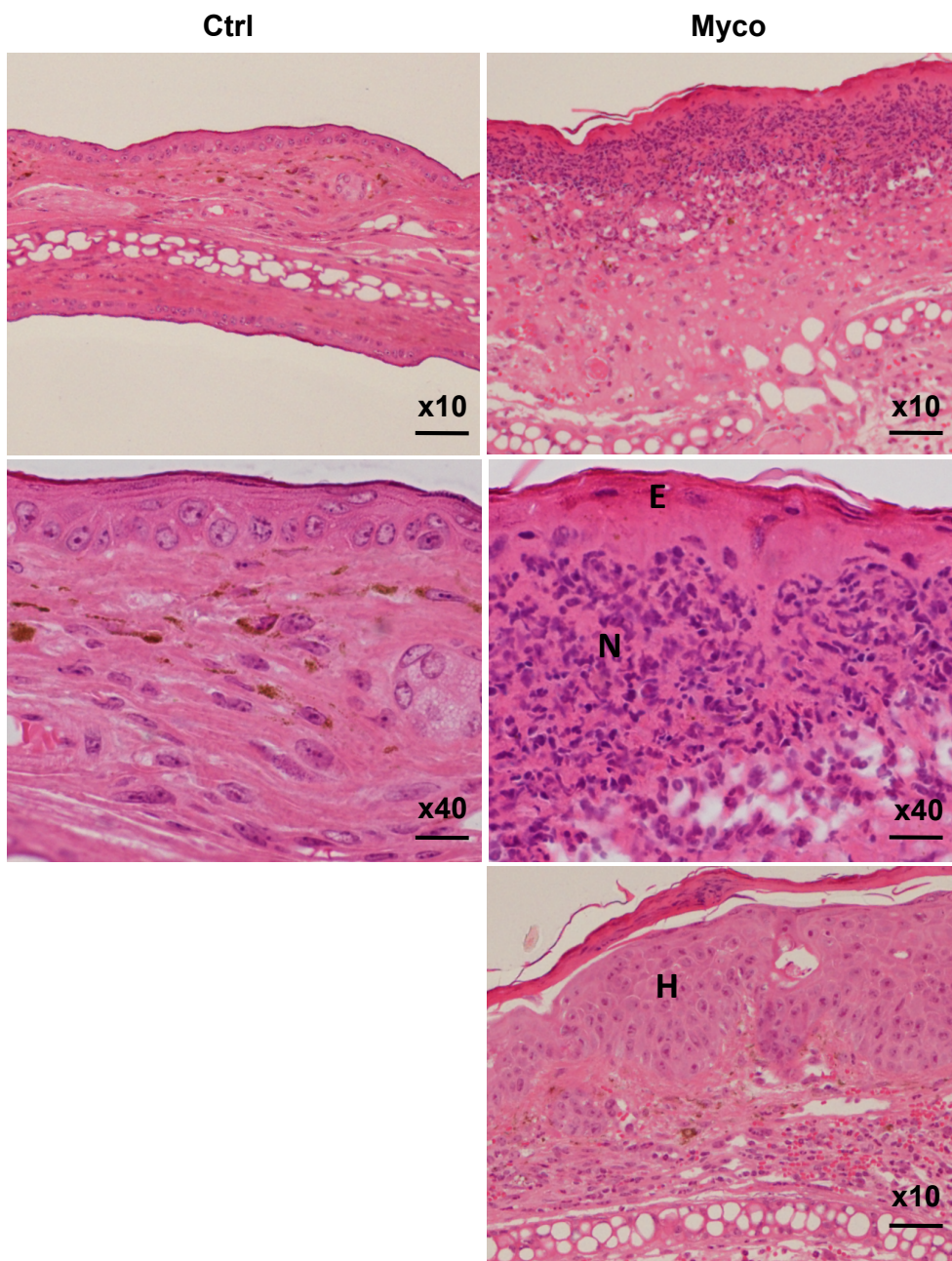
Estimation of the equilibrium dissociation constant K_d for the binding of mycolactone to N-WASp. The dependence of the increase in maximal rate of actin assembly on mycolactone concentration $[M_0]$ provides a measurement of the number of filament branching events generated at mid-polymerization by mycolactone-activated N-WASp with Arp2/3 complex. The data provide an indirect estimate of the binding of mycolactone to N-WASp at constant concentration $[W_0]$. The data were plotted in terms of a hyperbolic saturation curve :

$DV/DV_{\max} = (1/2[W_0]) \cdot \{ [W_0] + [M_0] + K \pm \{ ([W_0] + [M_0] + K)^2 - 4 [W_0] \cdot [M_0] \}^{1/2} \}$. The best fit of the data to the theoretical curve provided a K_d of 170 nM.



Supplemental Figure 4

Fluorescently-labeled and biotinylated mycolactone have comparable subcellular distributions. Jurkat T cells were incubated with 2 mM Bodipy-Myco for 1 h, then fixed for 20 min in paraformaldehyde 4% in PBS (left) or incubated with biotinylated-Myco for 1 h, fixed, then incubated for 1 h with anti-biotin polyclonal antiserum, and 45 min with anti rabbit IgG-Cy3 conjugate. Images were acquired on a Zeiss LSM700 with the x 40 immersion oil objective (Scale bar, 5 μ m). Pictures are views of a 1 mm focal plane.



Supplemental Figure 5

Remodeling of the epidermis by mycolactone. Hematoxylin/eosin staining of plastic-embedded 1 μ m sections of ear skin 9 days post intradermal injection of 7 nmol (5 μ g) mycolactone (Myco), compared to vehicle-treated controls (Ctrl) (Scale bar 10x, 50 μ m; 40x, 15 μ m). The Myco series of pictures illustrate the destruction of the epidermis (E) with polymorphonuclear infiltration (N) that characterize pre-ulcerative lesions, and the important epidermal hyperplasia (H) that is observed in the flanking regions.